Max-Planck-Institut für Metallforschung
Stuttgart

The Influence of Crystallization on the High Temperature Deformation Behavior of Precursor Derived Si-B-C-N Ceramics

Ravi Kumar N. V

Dissertation
an der
Universität Stuttgart

Bericht Nr. 171
Mai 2005

The Influence of Crystallization on the High Temperature Deformation Behavior of Precursor Derived Si-B-C-N Ceramics

Dissertation

Von der Fakultät Chemie der Universität Stuttgart

zur Erlangung der Würde eines

Doktors der Naturwissenschaften (Dr. rer. nat.)

genehmigte Abhandlung

Vorgelegt von

Ravi Kumar N. V
Aus Mysore, Indien

Hauptberichter : Prof. Dr. rer. nat. Fritz Aldinger

Mitberichter : Prof. Dr. rer. nat. Dr. h. c. mult. Günter Petzow

Prüfungsvorsitzer : Prof. Dr. phil. Eduard Arzt

Tag der mündlichen Prüfung : 30th May, 2005

Institut für Nichtmetallische Anorganische Materialien der Universität Stuttgart

Max-Planck-Institut für Metallforschung, Stuttgart

Pulvermetallurgisches Laboratorium

2005

Dedicated to my family members and to all my wellwishers and specially to my MUNNI

An important scientific innovation rarely makes its way by gradually winning over and converting its opponents: What does happen is that the opponents gradually die out.

- Max Karl Ernst Ludwig Planck
(1858 – 1947)

Acknowledgements

This Ph D work done was during the period, March 2001 to February 2004 at Max-Planck-Institute for Metals Research, Stuttgart, and was supported by a fellowship offered by the Max-Planck-Society which is gratefully acknowledged and I feel honored for the same. I would consider myself to be extremely fortunate to have worked in one of the premier research institutions of the world with excellent facilities for research and a nice working atmosphere. Pulvermetallurgisches Laboratorium (PML), the laboratory in which my Ph D work was carried out predominantly, is the epitome of fundamental research in the areas of *Materials Synthesis and Microstructure Design.* Its truly a wonderful experience working in this lab.

In my endeavor for this work, I have been scrupulously trained and moulded by my research supervisor, Prof. Dr. Fritz Aldinger, for which I am truly fortunate. Every discussion that I had with him has always been a pleasure, enlightening and educative, considering his wide knowledge and expertise in the subject. I express my warm and sincere heartfelt thanks for the *confidence he had shown, absolute freedom he had given and the vast amount of patience* he had with me.

I take this opportunity to thank Prof. G. Petzow who has consented to become the "Mitberichter" for my final examination. I also take this opportunity to thank Prof. E. Arzt for his consent to become the “Prüfungsvorsitzender” and who also has been kind enough to go through my thesis.

My special thanks to Dr. G. Rixecker, who consented to go through my thesis and offer useful suggestions. He has been kind enough to help me in all the administrative matters which made my life at MPI a comfortable one. I am grateful to him for all the pains that he has taken during my stay here solving my problems.

I would also like to thank my former group leader Dr. André Zimmermann for his initial advice and guidance in this topic of research. Dr. Y. Cai is gratefully acknowledged for carrying out transmission electron microscopy for all my samples without which, my thesis could not have been completed successfully, the discussions that I had with him have been quite useful.

Mr. Mager has been very helpful in carrying out all my experiments through out my stay at PML, without whose help, it would have been simply impossible to finish the work in time. My sincere gratitude and thanks for his support. Last but not the least, it would be a blunder if I do not thank Mr. Gerstel, who provided the precursor polymer for this research work. He has been quite helpful and very friendly which I would cherish for ever. Ms. Sabine Wolff (Prinz) has been very helpful and friendly during the first year of my stay, helping and teaching me the processing of polymer derived ceramics for which I am grateful. Thanks to Prof. Müller, Institute for Physical Chemistry, University of Stuttgart, and Dr. Frank Berger for the NMR results and the useful discussion that I had with them. My sincere thanks to Prof. Dr. –Ing. Grathwohl, Keramische Werkstoffe und Bauteile, University of Bremen, for the extremely useful discussion that I had with him.

There has been some useful discussions with Dr. Weinmann, Dr. Bill and Dr. Golczewski during my stay in PML and I gratefully acknowledge it.

I would also like to take this opportunity to thank Dr. Alexander Wanner (formerly department Arzt, MPI and presently Professor, University of Karlsruhe) for helping me to carry out the ultrasonic phase spectroscopy for my samples. I would like to thank Dr. Ulrike Wegst in helping me to carry out focused ion beam microscopy (FIB), but the work could not be completed due to time constraints.

Thanks to Dr. Fritz Phillip, department of Prof. Rühle for the useful discussions that I had with him.

There were many people at PML who made my research life simple and comfortable and full of fun. Mr. Kaiser, Ms. Schäfer, Mr. Labitzke, Ms. Thomas, should be acknowledged for their timely help in carrying out the chemical analyses, metallographic assistance, SEM and XRD respectively. Ms. Paulsen's smiling face can never be forgotten; she has been so nice and helpful during my stay in PML.

I would like to thank all my Indian friends at whose company made my life filled with joy and fun, the list is long. To mention a few, Narayan, Subasri, Datta, Koushik, Gautam, Manga from PML, Vinod, Mohapatra, Atul, Jay from Abt. Mittemeijer, Vijay, Nachi, Kailash, and Gourishankar from MPI/FKF. Among the international friends, I enjoyed the company of Shi

Jun Jia, Wang, Lee, Peng, Karin, Krenar, and Branco. If any names have been omitted, its simply unintentional and I thank every one for their support.

Contents

List of Figures

List of Tables

Chapter – 1

Introduction & Literature Review

1.1 Introduction

Precursor derived ceramics have been a focus of research interest in the last decade due to the extraordinary properties exhibited by these ceramics. High mechanical stability, chemical homogeneity, high thermal stability, good oxidation resistance accompanied by the ability to tailor the properties at the atomic level are a few highlights of this class of ceramics. In particular, extensive investigation has been carried out to design new polymer precursors to obtain high ceramic yields, and extensive phase studies have been done to understand the materials' phase stability. When a new group of materials is developed, it is always necessary to determine the properties of the material to evaluate its potential and the performance. When high temperature materials such as Si-B-C-N ceramics are developed contemporary to existing structural ceramics, with extraordinary properties as indicated above, an important mechanical property that would be looked for, is *creep resistance*.

The thesis starts with Chapter 1 with a brief literature review of existing high temperature materials and their properties. A review on typical materials usable at temperatures beyond that of superalloys such as Nb-based composites, Mo-Si-B based composites, platinum based metal alloys and SiC based composites gives an idea of the standing of precursor derived ceramics with respect to these materials. After a brief discussion on the high temperature deformation behavior of amorphous Si-B-C-N ceramics, the scope of the present investigation is outlined.

Nano-crystalline Si-B-C-N ceramics obtained from two different polymer precursors (MW-33 and T2-1) with different processing conditions were considered for investigation. The details on the processing of the polymer precursor, optimization and processing of dense ceramic monoliths derived from the polymer precursor are included in Chapter 2. This chapter also includes details on the techniques used for structural and mechanical characterization of these ceramic materials. The polymer-derived ceramics were investigated for their high temperature mechanical properties by carrying out compression creep experiments using two different

creep machines, from Amsler make and Zwick respectively. Hence the results obtained on the two types of materials investigated are discussed separately and treated in different chapters for clarity of data and interpretation of results (Chapter 3 and Chapter 4).

Si-B-C-N ceramics derived from the MW-33 polymer precursor were annealed under various conditions (temperature, N_2 overpressure and holding time are the variables) to produce crystalline Si-B-C-N ceramics with various microstructures revealing nano-sized structural features. The influence of the holding time and the nitrogen overpressure on the crystallization processes in the material was established. Structural characterization by X-ray diffraction (XRD), solid state nuclear magnetic resonance spectroscopy (NMR), and transmission electron microscopy (TEM) provide an insight into the crystallization processes. The high temperature deformation behavior of these nano-crystalline Si-B-C-N ceramics was investigated by carrying out constant load and load change experiments. Extensive load change experiments were carried out to investigate the creep viscosities at elevated temperatures and comment on the anelastic behavior observed in these materials. Samples obtained under two different processing conditions (with respect to the nitrogen overpressure: one obtained in a nitrogen atmosphere of 1 MPa and the other at 10 MPa were characterized at three different temperatures (1300 °C, 1350 °C and 1400 °C). The influence of the nitrogen overpressure on the crystallization behavior and henceforth on the high temperature deformation behavior is also discussed in Chapter 3.

In Chapter 4, the processing of Si-B-C-N ceramics derived from the polymer precursor T2-1, optimization details, annealing treatments and structural characterization of these crystallized samples by XRD, TEM and energy filtering transmission electron microscopy (EFTEM) are elucidated. This is followed by an investigation of the elastic properties of different crystallized materials as a function of annealing temperature, densities, and the initial polymer particles used, using ultrasonic phase spectroscopy. An attempt to establish the relation between the elastic properties and the annealing temperature and density is made.

Subsequently, this chapter is also focused on the investigation of the compressive creep behavior of nano-crystalline Si-B-C-N ceramics from T2-1 precursor obtained at different annealing temperatures (1800 °C and 1900 °C). The investigation highlights the deformation behavior at elevated temperatures for nano-crystalline ceramics obtained at different annealing temperatures and considers the influence of oxygen contamination.

1.2 Literature review: High Temperature Materials

1.2.1 Overview

This section focuses on reviewing the existing high temperature structural materials and reasoning out the choice of the present material for investigation. Development of new materials for high temperature applications has always been a subject of challenge and interest for material scientists. The stringent conditions the materials in high temperature applications are subjected to, and the ever increasing demand to maximize the performance of the materials used in aerospace industries, automobile industries and so on, is the driving force for further research in this area of high temperature structural materials.

For example, J.-C. Zhao and J. H. Westbrook [03Zha] recently reviewed the available ultrahigh temperature materials for jet engines. A jet engine is quite complex, yet operationally a simple device, the efficiency and the performance of which is strongly dependent on the highest temperature in the engine-the inlet temperature of the HPT (high pressure turbine vanes) - and it is the high temperature capability of these parts that is critical. To achieve higher thrust, higher operating temperatures must be realized. To achieve higher efficiency, engines must be made significantly lighter without loss of thrust. In either case, it is obvious that a completely new class of materials must be developed, ones with higher melting points and greater intrinsic strengths.

A bird's eye view of the existing high temperature materials with their relative merits and demerits, gives an idea about each class of high temperature materials. The materials that

could be considered on a broad scale are superalloys, refractory metals, monolithic ceramics, intermetallic compounds and composites [03Zha].

Superalloys are a group of alloys based on Group VIIIB elements and usually consist of various combinations of Fe, Ni, Co, and Cr, as well as lesser amounts of W, Mo, Ta, Nb, Ti, and Al. The three major classes of superalloys are nickel-, iron-, and cobalt-based alloys. They were developed for use in turbosuperchargers and aircraft turbine engines that required high performance at elevated temperatures. They are particularly well suited for these demanding applications because of their ability to retain most of their strength even after long exposure times above 650 °C. Their versatility stems from the fact that they combine this high strength with ductility and oxidation resistance. Although nickel based superalloys melt at about 1250 °C they are supposed to be operating at 85 % of their melting point. However, above temperatures around 1000 °C, they tend to be susceptible to environmental attack because of the presence of reactive alloying elements (which provide their high-temperature strength). Surface attack includes oxidation, hot corrosion, and thermal fatigue.

For higher temperature applications, intermetallics and refractory metals have attracted attention. Although intermetallics are lighter than nickel, they do not offer significantly higher temperature capability and refractory metals such as tantalum, niobium, molybdenum, and tungsten suffer from poor oxidation resistance. All of them with the exception of chromium are substantially heavier than the present-day Ni-based alloys. Though chromium has the advantage of being lighter than nickel, it is marginally tough at room temperature and is subject to nitrogen embrittlement when exposed to air at high temperatures. Platinum group metal alloys (PGM alloys) do show good properties, but suffer from poor thermal shock resistance and high cost.

Nb silicide composites, Mo-Si-B composites, and SiC/SiC ceramic matrix composites are some of the non-metallic candidates for high temperature use. Nb silicide composites show good oxidation resistance, good high temperature strength, but combining high oxidation

resistance with high strength is a major problem. Mo-Si-B composites on the other hand, exhibit excellent high temperature creep strength, and good oxidation resistance above 1000 °C. But these composites suffer from poor impact resistance and low fracture toughness [03Zha].

According to R. Raj [93Raj], structural ceramics for high temperature applications should embody the following properties: oxidation resistance, chemical stability, low volatility, resistance to creep deformation, resistance to creep cavitation at interfaces, sufficient toughness at ambient temperatures and thermal shock resistance. Due to their favorable fracture mechanical behavior liquid phase sintered silicon carbide and nitride are obvious choices in the ceramics category. They have been subjected to extensive research already for quite long and the deformation processes in these materials at elevated temperatures are now reasonably well understood [02Pet]. The less refractory oxidic grain boundary phase in these materials, which results from the liquid phase sintering process, is a serious set back from better creep properties, as it is the first phase to deform at elevated temperatures bringing down the effective creep resistance of the material. Wiederhorn *et al.* [99Wie] compared the relative merits of liquid phase sintered β-Si_3N_4 with solid state sintered α-SiC for high temperature applications. It was shown that the liquid phase sintered β-Si_3N_4 was not as creep resistant as it contained a residual sintering aid at its grain boundaries that deforms at a much lower temperature than the silicon nitride grains themselves. As a new direction in the high temperature materials research newly developed, polymer derived ceramics in systems such as Si-C-N and Si-B-C-N which have high thermal stability and which could offer better mechanical properties at elevated temperatures have been a topic of research interest during the last decade [95Bil, 00Wei]. This is possible since these materials are processed without any sintering aids and lack any oxidic grain boundary phases.

1.2.2 Precursor derived ceramics

The use of organometallic precursors which can be transformed to amorphous covalent ceramics at temperatures around 1000 °C has recently attracted wide attention. Although known for about 70 years, only the pioneering work of Verbeek and Winter [73Ver, 74Ver] as well as Yajima [75Yaj1, 75Yaj2, 76Yaj] in the mid 1970s focused on the fact that ceramics can be produced from polymeric precursors. With polymeric precursors, advantages can be taken from the use of polymer forming techniques, enabling (i) the preparation of ceramic powders via spray pyrolysis, (ii) the use as binders in injection moulding, (iii) the preparation of melt spun or dry spun fibers, (iv) coatings, or (v) the formation of ceramic matrices via infiltration of fibrous performs or porous structures.

In general, the processing of ceramic materials through organometallic precursors involves the synthesis of preceramic thermosetting polymers or oligomers from monomeric units, followed by crosslinking these polymers in order to obtain an unmeltable preceramic network, enabling high ceramic yields and shape stability. Transformation of the cross linked precursors into amorphous covalent ceramic materials is performed by heat treatment in inert atmospheres. It should be emphasized that the polymeric network is locally reconstructed during the organic-inorganic transition forming new bonds. Post-annealing of amorphous materials at higher temperatures yields crystallization of the corresponding thermodynamically expected equilibrium phases. The crystallization temperature depends on the structure and constitution of the amorphous phase. One of the important issues regarding multi-component precursor derived ceramics is the thermal stability, i.e., the stability of the amorphous structure, in particular.

Out of the many precursors, organosilicon precursors are of interest which can be used for silicon containing ceramics. A review on precursor derived ceramics [95Bill, 00Wei] demonstrates some recent developments in the field of the synthesis of covalent ceramics such as carbides and nitrides by pyrolysis of preceramic compounds, in which it is said that

the architectural design of advanced ceramics based on atomic or molecular units is an ideal way of controlling structure and properties. Using this process, high purity products with a homogeneous distribution of the elements on an atomic scale and controllable microstructures can be obtained at relatively low temperatures.

1.2.3 Si-B-C-N ceramics: Thermal stability and thermodynamics

The development of materials in the Si-B-C-N quaternary system is an important advancement in high temperature materials research. Pyrolysis of polysilazanes in an inert atmosphere around 1000 °C yields ternary Si-C-N ceramics. Si-C-N materials decompose at 1400 °C – 1500 °C in nitrogen and nitrogen-free environments due to the decomposition of Si_3N_4 in the presence of excess carbon. Precursor-derived silicoboron carbonitride (Si-B-C-N) materials have noticeably higher thermal, chemical, and mechanical stability than boron-free Si-C-N materials at very high temperatures.

The addition of boron to the ternary system increases the thermal stability to the order of 1800 °C – 2000 °C, which makes these materials more interesting and worth investigating. The microstructure development of monolithic Si-P-C-N and Si-B-C-N ceramics synthesized by Bill *et al.* [95Bill] showed that the alternative addition of phosphorus gives a rather coarse overall microstructure after heat treatment. On the other hand, addition of boron increases the crystallization temperature and favors the formation of a fine grained microstructure with both the constituents being of the order of a few tens of nanometres in size. Moreover, these authors observed a thin coating of BN covering the crystallites and concluded that the marked decrease in the crystallite size is because of BN diffusion barriers limiting grain growth. Thus boron not only acts as a nucleation inhibitor but also inhibits grain growth. Since amorphous precursor derived ceramics are free from grain boundaries, it was argued that the mechanical properties in the amorphous state should be better than of those obtained from conventionally sintered materials.

Thermodynamic calculations carried out by Peng *et al.* [02Pen], showed that these ceramics should be composed of Si_3N_4, SiC, BN and graphite at temperatures below 1484 °C. Above 1484 °C Si_3N_4 should react with graphite to form silicon carbide and gas and the total mass of the ceramic should decrease due to the loss of gaseous N_2. However, experimental observations indicated that some of these ceramics exhibit no major mass loss up to temperatures around 2000 °C or even higher. Peng *et al.* also showed that the XRD patterns of ceramics derived from the polymer T2-1 (see section 2.2) still consisted of β-Si_3N_4 besides β-SiC and BNC even after heating up to 2200 °C, although Si_3N_4 should have decomposed under these conditions according to the calculated results. HRTEM investigations of these materials showed that the crystallites were embedded in a turbostratic matrix of BNC [96Jal]. By NMR, carbon not bound to silicon is found in the turbostratic phase (BNC), whose structure is thought to be related to both graphite and hex-BN. Because of this structure, carbon is passivated, i.e., its activity is significantly reduced and its reaction with Si_3N_4 inhibited.

To derive quantitative information on the effect of decreased carbon activity, the carbon activity vs. temperature diagram was calculated by the aforementioned authors [02Pen]. At a pressure of 0.1 MPa N_2 the temperature of the reaction between Si_3N_4 and carbon is increased from 1484 °C to 1841 °C by decreasing the carbon activity from 1 to 0.1 At even lower carbon activities Si_3N_4 decomposes in to liquid silicon and nitrogen as shown on the left hand side of the diagram.

Under the same conditions, the reaction temperature between Si_3N_4 and carbon at the higher nitrogen pressure of 1 MPa increases from 1700 °C to 2034 °C. It has to be emphasized that the absolute pressure values and activities in the Si-B-C-N ceramics are not known exactly, but the Figure 1.1 shows quantitatively the increase of stability of Si_3N_4 by pressure increase and carbon activity reduction which may be induced by the specific microstructure. Zhi-Chang Wang *et al*. [01Wan] also report on the thermal stability of Silicon-Boron Nitrogen-

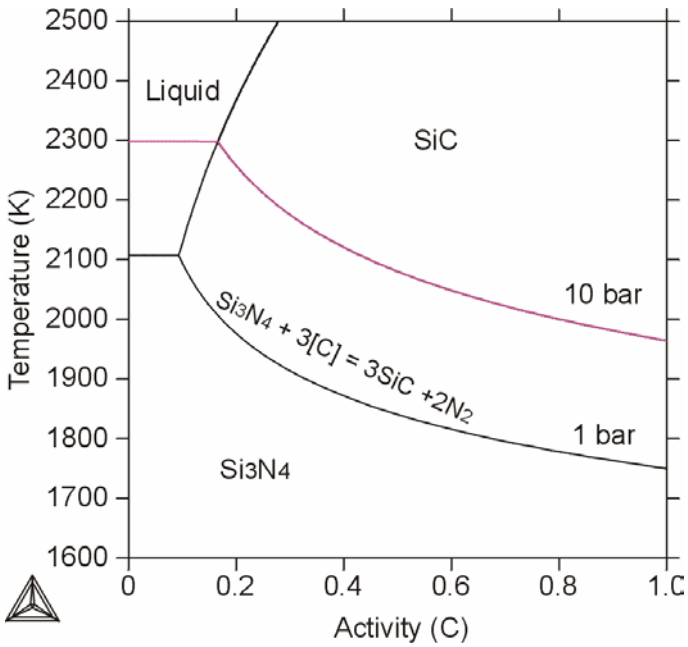

Figure: 1.1 Carbon activity vs. temperature diagram [02Pen].

Carbon materials. Three novel Si-C-B-N ceramic compositions, namely $Si_{2.9}$ $B_{1.0}$ C_{14} $N_{2.9}$, $Si_{3.9}$ $B_{1.0}$ C_{11} $N_{3.2}$ and $Si_{5.3}$ $B_{1.0}$ C_{19} $N_{3.4}$, were synthesized using the polymer-to-ceramic transformation of the polyborosilazanes $[B(C_2H_4Si(Ph)NH)_3]_n$, $[B(C_2H_4Si(CH_3)NH)_2–(C_2H_4Si(CH_3)N(SiH_2Ph))]_n$, and $[B\text{-}(C_2H_4\ Si(CH_3)–N(SiH_2Ph))_3]_n$, where Ph is phenyl ($C_6H_5$), at 1050 °C in argon. The Si-B-C-N ceramics exhibited significant stability with respect to composition and mass change in the temperature range between 1000 °C and 2200 °C, including isothermal annealing of the samples at the latter temperature for 30 min in argon. The mass loss rate at 2200 °C was as low as 1.4 wt %/h for $Si_{5.3}$ $B_{1.0}$ C_{19} $N_{3.4}$, 1.7 wt %/h for $Si_{2.9}$ $B_{1.0}$ C_{14} $N_{2.9}$, and 2.4 wt %/h for $Si_{3.9}$ $B_{1.0}$ C_{11} $N_{3.2}$. The measured mass loss rate was comparable to that of pure SiC materials. As crystalline phases, β-Si_3N_4 and β-SiC were found exclusively in the samples annealed at 2200 °C at 0.1 MPa in argon. For thermodynamic reasons, β-Si_3N_4 should have decomposed into the elements silicon and nitrogen at that particular temperature and gas pressure. However, the presence of β-Si_3N_4 in these materials indicated that carbon and boron kinetically stabilized the Si_3N_4 based composition. All the Si-B-C-N materials known so far contain excess carbon with respect to

their thermodynamically stable binary phases, namely SiC, BN, and Si_3N_4. Thus, the crystallization and subsequent decomposition of Si-B-C-N materials at T = 1450 °C under 0.1 MPa nitrogen pressure would be expected to follow Equations 1.1 and 1.2:

$$4Si_x B_{1.0} C_y N_z = 4BN + (z - 1)\beta\text{-}Si_3N_4 + (4x + 3 - 3z)\beta\text{-}SiC + (4y + 3z - 4x - 3)C \quad (1.1)$$

$$\beta\text{-}Si_3N_4\,(s) + 3C\,(s) = 3\beta\text{-}SiC\,(s) + 2N_2\,(g) \quad (1.2)$$

However, in the course of their work, Wang *et al.* [01Wan] found no significant changes in mass or composition after annealing of the as-synthesized amorphous Si-B-C-N materials up to 2200 °C in 0.1 MPa argon. Instead, the presence of Si_3N_4, even after heating the samples at 2200 °C in nitrogen, indicates that carbon and boron kinetically stabilize distinct Si-B-C-N compositions. This observation agrees with a theoretical study based on molecular dynamics simulations, where the self-diffusion coefficients of Si-B-C-N were calculated [99Mat, 01Mat]. The authors were able to demonstrate that carbon and boron enforce a stabilizing effect on Si_3N_4. The self-diffusion coefficients of nitrogen and carbon decrease with increasing boron content, while that of silicon is decreased by increased amounts of carbon. Decreased atomic diffusivities of the constituent elements silicon, carbon, and nitrogen correspond with an enhanced thermal stability of amorphous Si-B-C-N.

1.3 Fundamentals of creep

Creep is a phenomenon where the plastic deformation of a material takes place when the material is subjected to a stress, well below its yield limit, at high homologous temperatures. Creep deformation can usually be subdivided in to three stages, namely, primary creep which is characterized by a decreasing strain rate, steady state or secondary creep which is characterized by a constant strain rate, and tertiary creep, which is characterized by increasing strain rates until failure. The qualitative behavior of the strain vs. time curve can be seen in Figure 1.2.

1.3.1 Creep asymmetry

Ceramics, unlike most metals, show directional anisotropy during high-temperature deformation. Therefore, creep-test results for tension will differ from those in compression. At the same temperature and applied stress, Si_3N_4 can creep 100 times faster in tension than in compression. In compression, the creep rate is usually linearly proportional to the applied stress. By contrast, creep in tension is distinctly non-linear, and recent investigations suggest an exponential dependence of the creep rate on the applied stress [00Yoo, 99Lue].

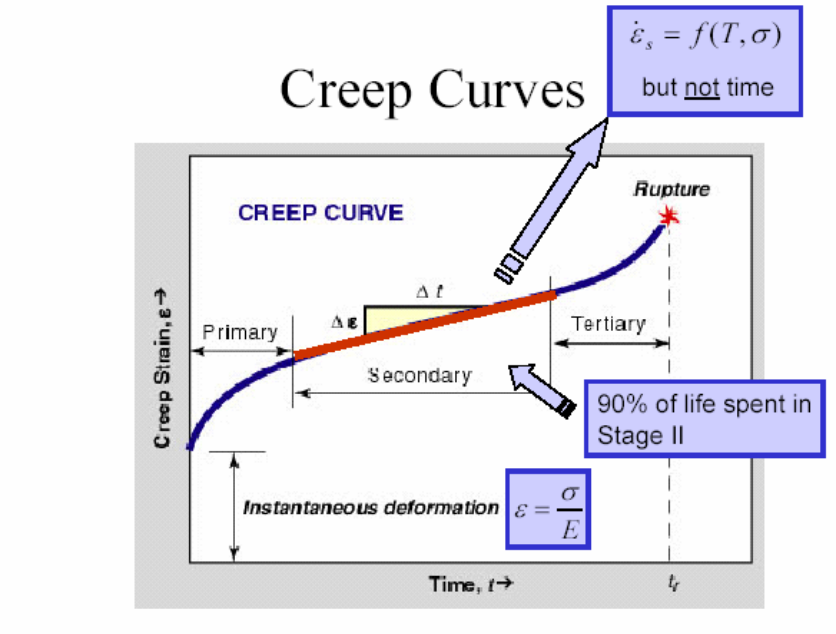

Figure: 1.2 Typical creep curve exhibiting all three stages of creep obtained during a long term creep test.

Creep asymmetry was first observed by Morrel and Ashbee [73Mor] in a lithium zinc silicate glass-ceramic which has the microstructure of a particulate-reinforced composite. Approximately two to six times as much stress was required in compression than in tension to achieve the same creep rates. This creep asymmetry is often accompanied by a change in stress exponent with applied stress. Hence it is always required to mention the kind of loading the material has been subjected to at elevated temperatures when the deformation mechanisms are discussed for a combination of temperature and stress.

1.3.2 High temperature deformation of amorphous ceramics

Amorphous ceramics in the Si-C-N and Si-B-C-N systems were investigated earlier which indicated high creep resistance at elevated temperatures [98Lin, 98Rie, 99Thu, 02Bau, 02Zim]. Thurn *et al.* [99Thu] investigated Si-C-N materials derived from polyvinylsilazane (PVS) and polyhydridomethylsilazane (PHMS) precursors in the temperature range between 1200 and 1550 °C at compressive stresses between 30 and 250 MPa in air. Decreasing strain rates with time were observed for both the materials which showed similar behavior and even after 4×10^6 s of creep deformation, stationary creep was not observed. During an entire compression creep test of amorphous Si-C-N precursor ceramics, Bauer *et al.* [02Bau] reported that the creep rates decrease by about two orders of magnitude with no approach to steady state between 1350 °C and 1500 °C and constant stresses ranging from 5 MPa to 300 MPa. There are reports of compression creep studies of Si-C-N ($Si_{1.7}\ C_{1.0}\ N_{1.5}$) and Si-B-C-N ($Si_2\ B_{1.0}\ C_{3.4}\ N_{2.3}$) exhibiting a three stage creep behavior in less than 15 ks of testing time. In stage I, the creep rate declined because of densification, and in stage II the creep rates approached a steady state. Stage III was characterized by further decrease in strain rates, which continued below the limit of the measuring system [98Lin, 98Rie]. However, such a three stage creep behavior was not reported by other authors in the amorphous Si-(B)-C-N systems.

Extensive creep studies in compression in the temperature range of 1350 °C – 1500 °C and at loads varying from 5 – 300 MPa for amorphous Si-B-C-N for nearly 300 h revealed only a primary stage creep [00Chr]. The absence of low melting point grain boundary phases in these materials leads to very good mechanical properties at elevated temperatures. Si-B-C-N ceramics obtained from the boron modified poly(vinyl)silazanes with chemical compositions of $(B[C_2H_4\text{-}Si(CH_3)NH]_3)_n$ (denoted T2-1) and $(B[C_2H_4\text{-}Si(H)NH]_3)_n$ (denoted MW-33) were investigated.

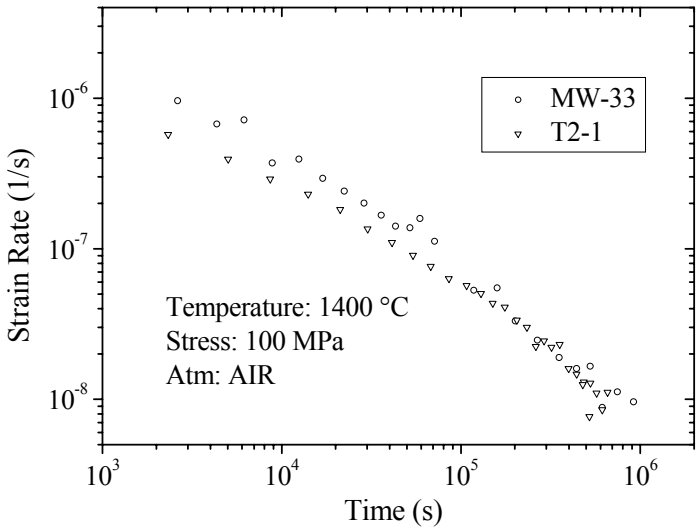

Figure: 1.3 Deformation of amorphous MW-33 and T2-1 derived Si-B-C-N ceramics during a 300 h compression creep test.

The deformation rates achieved at the end of 300 h (~ 10^6 s) in a typical compression creep test carried out at 1400 °C at 100 MPa for both MW- 33 and T2-1 derived amorphous Si-B-C-N ceramics was on the order of < 10^{-8} /s (Figure 1.3). The total deformation accumulated in 100 h creep tests was typically 2 % - 5 %. This was found to be dependent on the applied stress but independent of precursor from which the material was derived.

Si-B-C-N ceramics in the amorphous state were extensively investigated by Christ *et al.* [00Chr] by carrying out creep studies in compression. It was shown that the deformation behavior of such precursor derived amorphous Si-B-C-N ceramics was similar to that of metallic glasses. In this respect, the applicability of deformation models used to describe the deformation behavior of metallic glasses was discussed for amorphous Si-B-C-N ceramics.

The experimental data were analyzed using two theoretical models, namely, the "*two-step rearrangement model*" and the "*free volume model*", both of which predict a linear variation of viscosity with time according to the following equation:

$$\eta(t,T) = a(T) + b(T)\, t\ , \qquad (1.3)$$

where, the viscosity is given by $\eta = \frac{\sigma}{3 \cdot \dot{\varepsilon}}$, with σ = applied stress and $\dot{\varepsilon}$ = strain rate (see Equation 3.3).

According to the two step rearrangement model, the deformation behavior is explained by structural relaxation of the material via non-correlated, two-stage, shear atomic rearrangements. An atomic rearrangement in a certain activation volume initiates the viscous flow of the surrounding region of volume Ω, and the deformation rate for low stresses is approximated as

$$\varepsilon'(\sigma, T, t) \approx \frac{\sigma k T N_0 \Omega C}{t + \tau}, \tag{1.4}$$

where τ = preannealing time at the creep test temperature T, t = creep time, k = Boltzmann constant, N_0 = volume spectral density of relaxation centers, and C = parameter that allows for the orienting effect of the applied stress on the atomic rearrangements in the relaxation centers. However, with the above relationship for the viscosity, Equation 1.4 can be transformed to:

$$\eta(T, t) \approx \frac{\tau}{3 k T N_0 \Omega C} + \left(\frac{1}{3 k T N_0 \Omega C} \right) t \tag{1.5}$$

which is a linear function of time similar to Equation 1.3 .

According to the free volume model, atomic transport for structural rearrangement is caused by flow defects that are formed by fluctuations in the distribution of the free volume in the amorphous material. These defects are also available for atomic transport during deformation. The deformation rate according to this model is given by:

$$\varepsilon' = 2 C_f k_f \frac{\gamma_0 \nu_0}{\Omega} \sinh\left(\frac{\sigma \gamma_0 \nu_0}{2 k T} \right) \tag{1.6}$$

where, C_f = concentration of flow defects, k_f = jump frequency of a flow defect or the rate factor for the thermally activated process of structural relaxation , γ_0 = shear strain per jump of a single flow defect, ν_0 = volume of one defect, and Ω = atomic volume.

According to Duine *et al*. [92Dui], the rate of change of the defect concentration far from equilibrium can be described as the net result of generation and annihilation of defects, such as:

$$\frac{dC_f}{dt} = -C_f k_f \left(C_f - C_{f,eq}\right) \tag{1.7}$$

where $C_{f,eq}$ is the defect concentration in thermal equilibrium.

The above equation also assumes that the thermal annihilation rate of defects is proportional to C^2_f, whereas the thermal defect production rate is proportional to C_f. Furthermore, it is assumed that the activation energy for the movement of the flow defects and the activation energy for the production of flow defects are equal. Hence, the viscosity in the free volume model takes the form

$$\eta(T,t) = \left[\frac{KT}{C_{f0}} \exp\left(\frac{Q}{RT}\right)\right] + (KC_0 T)t \tag{1.8}$$

where $K = \frac{k\Omega}{(\gamma_0 \nu_0)^2 \nu_0}$, C_{f0} and C_0 are constants, C_{f0} representing the starting value of the concentration of flow defects. This means that the viscosity in the frame work of free volume model is also a linear function of time.

It was shown that the time dependence can be well predicted by both models, unlike the temperature dependence. It was observed by Christ *et al.* [00Chr], that though the viscosity varied greatly for shorter times, it became independent of temperature at longer times ~ 3 x 10^5 s. From this observation it was concluded that the a(T) term in Equation 1.3 is much more dependent on temperature than the b(T) term. If the quantity a(T) is temperature dependent as the inverse of temperature 1/T, as it is predicted by the two-step rearrangement model, the plot of a vs. 1/T should be a straight line. Using the experimental data of amorphous Si-B-C-N ceramics, however, the plot of a vs.1/T was found to be clearly non-linear. This fact was accepted as a rejection of the two-step rearrangement model. On the other hand, it was noted

that the plot of a vs.1/T was consistent with the prediction of the free volume model. Hence it was concluded that the temperature dependence of the viscosity of amorphous Si-B-C-N ceramics can be better explained via a free volume model. With this analogy, it was shown that the deformation behavior of amorphous Si-B-C-N ceramics at elevated temperatures is similar to that of metallic glasses.

1.3.3 Crystallized Si-B-C-N ceramics

Preliminary studies on crystallized Si-B-C-N ceramics carried out by Christ *et al.* [01Chr], showed an interesting potential of these materials. For crystallization, amorphous precursor derived Si-B-C-N ceramics were annealed at 1800 °C for 3 h in a nitrogen atmosphere of 1.5 MPa, which yielded a material consisting of α/β SiC with a mean grain size of about 100 nm embedded in a turbostratic matrix containing BN and C. The deformation behavior of this material was investigated by carrying out compression creep studies at 1400 °C in air. The deformation rate consisted of a component proportional to the applied stress, indicating a viscous flow based deformation mechanism. As in the case of amorphous Si-B-C-N ceramics, Christ *et al.* [00Chr] found that the strain rate decreased continuously to extremely small values (~ 10^{-8} s^{-1}) without approaching a steady state value. Hence the deformation behavior of crystallized Si-B-C-N ceramics was analyzed along similar lines as that of their amorphous counterparts. It was observed that the deformation behavior was qualitatively the same for both amorphous and crystallized ceramics. But the strain rates of the crystallized ceramics at 100 MPa and 1400 °C were found to be just 20 % of the strain rates that are observed for amorphous materials under the same conditions.

1.4 Scope of the present investigation/motivation for the present work

Until now, amorphous materials in the Si-B-C-N system have been investigated for their high temperature mechanical properties and have shown interesting potential. In particular, the

investigation of amorphous Si-B-C-N ceramics with respect to their compressive creep behavior has been very extensive. Several reasons can be given as a motivation to carry out the present investigation, namely:

- Amorphous Si-B-C-N ceramics are thermodynamically metastable and upon annealing, crystallites of the equilibrium phases SiC and Si_3N_4 are formed beside turbostratic BNC_X. Hence an investigation of these materials after such stable phases have formed is interesting and worthwhile for comparison.
- Preliminary investigations of crystallized precursor derived Si-B-C-N ceramics indicate that the creep resistance increase by crystallization. Upon in situ crystallization of metallic glasses, it was found that the creep resistance increases even several orders of magnitude [80Pat]. Hence it is interesting to investigate the potential of crystallized Si-B-C-N ceramics in more detail.
- Crystallization provides nano-scaled grain sizes. A systematic detailed study of the influence of crystallization on the creep behavior will provide an understanding of the deformation mechanisms in such nano-crystalline Si-B-C-N ceramics.

Chapter – 2

Experimental

Nano-crystalline Si-B-C-N ceramics obtained from two different polymer precursors (MW-33 and T2-1) were considered for investigation. The details on the processing of the polymer precursor, optimization and processing of dense ceramic monoliths are described in the following sections. This chapter also includes details on the techniques used for structural and mechanical characterization of these ceramic materials.

2.1 MW-33 polymer derived materials

2.1.1 Polymer synthesis and pyrolysis

The detailed description of the synthesis of the polymer precursor, boron modified polyvinylsilazane with a chemical composition $(B[C_2H_4\text{-}Si(H)NH]_3)_n$, can be found elsewhere [00Wei]. In brief the synthesis of the polymer follows the reaction shown Figure 2.1.

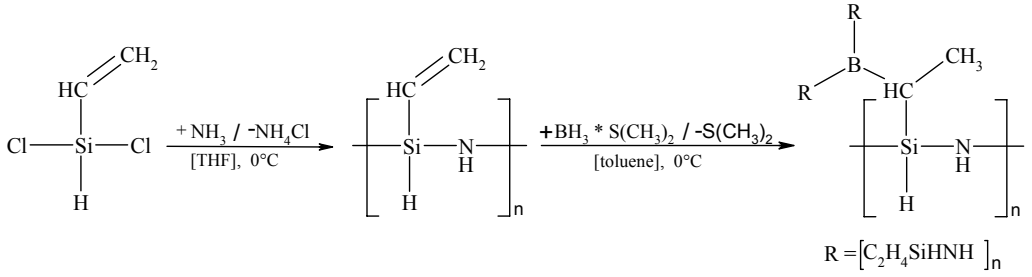

Figure: 2.1 Synthesis of the polymer precursor MW-33.

Subsequently the polymer is dried carefully at 120 °C and 0.1 Pa for several days. From this treatment one receives highly cross-linked polymer lumps. The total synthesis is carried out in argon or nitrogen atmosphere to prevent contamination by oxygen of the polymer. The elemental analysis of the synthesized polymer is shown in Table 2.1.

As seen in the table, the values obtained from the chemical analysis of the polymer do not substantially vary from the theoretical calculation. Hence it can be inferred that the polymer is obtained with the desired structure based on the formula indicated in Figure 2.1 substantiating the possibility of designing the polymer at the atomic level.

	Si	C	N	B	H	O
Theoretical calculation	37.07	31.71	18.49	4.75	7.98	0.00
Chemical Analysis						
Batch - I	35.90	31.60	19.30	4.55	7.75	1.50
Batch - II	34.00	31.06	20.30	4.60	7.40	1.20
Batch - III	34.20	34.30	15.70	5.00	8.40	2.00

Table: 2.1 Comparison of the elementary composition (in mass %) of different batches of the polymer MW 33 with calculated values.

After crosslinking, the polymer lumps are pulverized using a tungsten carbide ball mill and the polymer particles are segregated into various size fractions by sieving. The different batches are thoroughly mixed for further processing. Table 2.2 provides details of the polymer particles used for compaction into green bodies.

	Size fraction [µm]	weight [g]
1	180 – 200	5.7
2	160 – 180	6.2
3	100 – 160	39.1
4	32 – 100	48.5
5	<32	21.7

Table: 2.2 Polymer particles size fraction used to prepare bulk ceramic bodies.

2.1.2 Warm pressing & thermolysis

The polymer particles as described above were compacted by uni-axial warm pressing in the temperature range 150 °C – 350 °C in a graphite die applying a pressure of 48 MPa in argon atmosphere. The obtained green body was subjected to solid state thermolysis at temperatures of 1300 °C – 1400 °C for 2 h in argon atmosphere with a heating rate of 1 K/min and a

cooling rate of 5 K/min. By thermolysis the polymer is converted to an inorganic network which is accompanied by gas evolution due to the removal of organic groups. The thermolysis program is as shown in Figure 2.2 (a). The samples pyrolyzed at 1400 °C showed traces of nano-crystallites of Si_3N_4 2-5 nm in size distributed in an amorphous matrix (Figure 2.2 (b)). The matrix is at least partially made up of turbostratic boron nitride and carbon. The objective was henceforth to produce a purely amorphous Si-B-C-N ceramic to start with, which is free of any traces of nano-crystallites. This was the reason for reducing the pyrolysis temperature to 1300 °C. Pyrolyzing the polymer green compacts at this temperature provides samples with no crystallites of Si_3N_4 and SiC and very less indication of the turbostratic phase (Figure 2.2 (b)).

The warm pressing of the polymer particles into a green compact was carried out using two different kinds of graphite punches. It was observed that the bulk bodies that were produced using a pair of flat punches had radial and axial cracks. Hence in order to avoid such kind of cracks in the samples, a punch which is concave and which provides a component of isostatic pressure was used. With the introduction of this concave punch, it was possible to produce crack free amorphous ceramics as shown in Figure 2.3 (b) which were also denser. Further analysis the crack free ceramics have been cut in to two parts using a diamond cutting wheel for further analysis.

The amorphous Si-B-C-N ceramics were crystallized at 1800 °C under a nitrogen overpressure ranging from 1 – 10 MPa and holding times of 1 to 3 h to study the effect of nitrogen overpressure and holding time on the crystallization behavior. Four different crystallized materials were synthesized by using the following conditions: (a) 1800 °C, 1 h -1 MPa N_2 , (b) 1800 °C, 1 h - 10 MPa N_2 , (c) 1800 °C, 3 h - 1 MPa N_2 , (d) 1800 °C, 3 h – 10 MPa N_2 respectively.

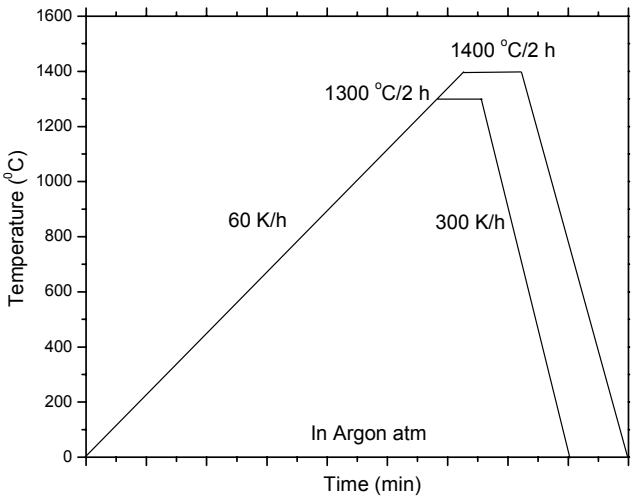

(a)

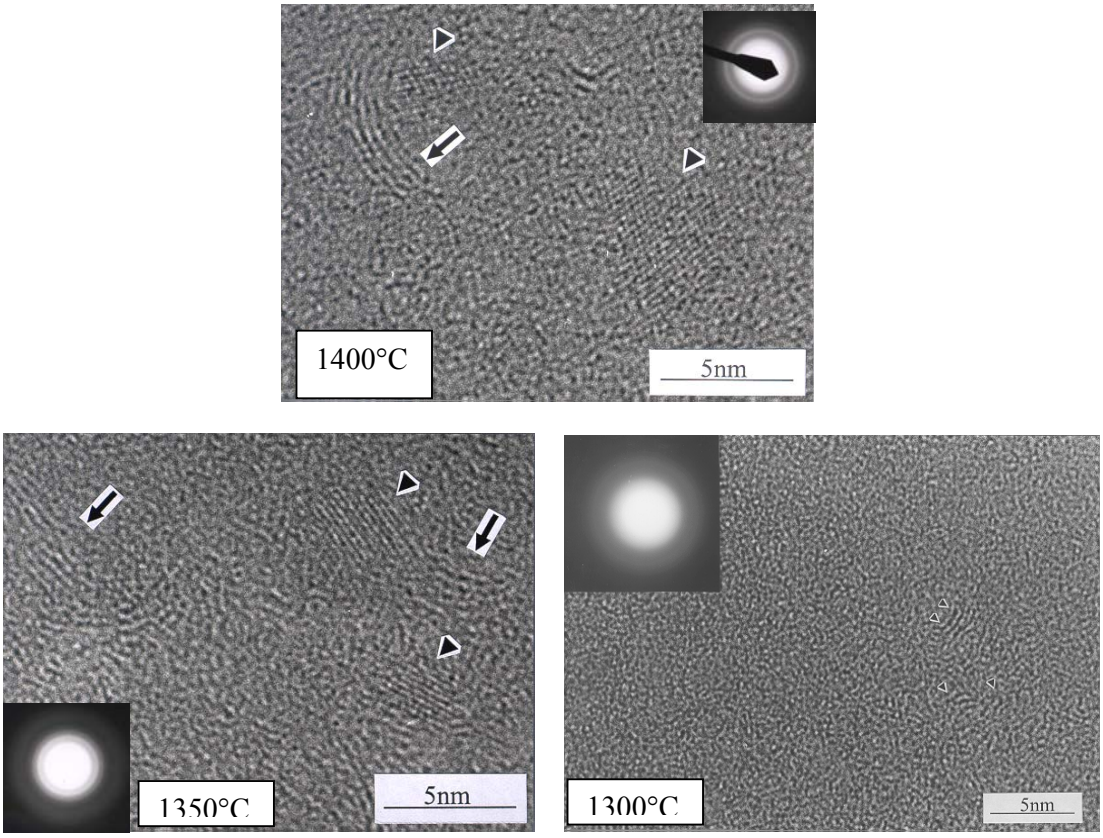

(b)

Figure: 2.2 (a) Pyrolysis program (b) TEM images of samples pyrolysed at 1400 °C, 1350 °C, and 1300 °C. Symbols denote nanocrystallites of Si_3N_4 (▶) and the turbostratic matrix containing B, C, and N (⟶).

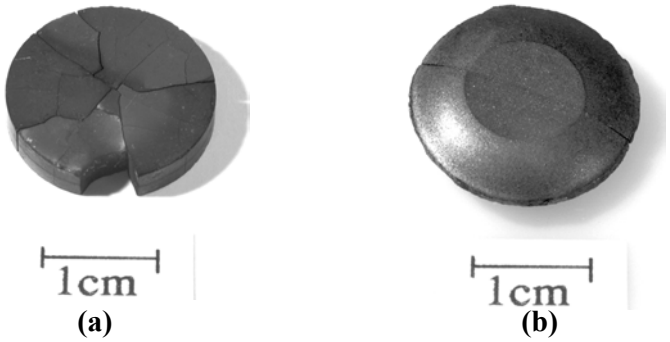

Figure: 2.3 Pyrolyzed amorphous Si-B-C-N ceramics produced using a flat punch (a) and a concave punch (b) for green compaction.

2.2 T2-1 polymer-derived materials

2.2.1 Synthesis of the polymer precursor T2-1

The polyborosilazane T2-1 was prepared according to Riedel *et al.* [96Rie] by a two step synthesis as shown in Figure 2.4 (Scheme **1**). First, the hydroboration of dichloromethylvinylsilane leads to tris(dichloromethylsilylethyl)borane **(1)**, second, the ammonolysis of **(1)** leads to the polyorganoborosilazane **(2).**

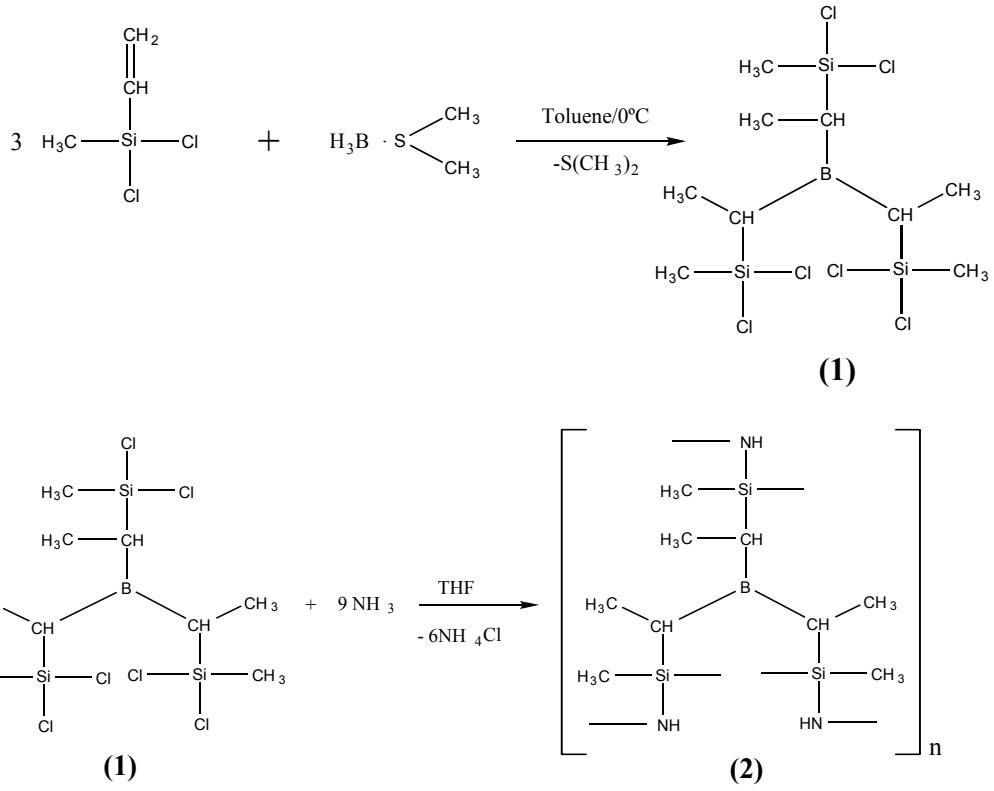

Figure: 2.4 Polymer synthesis procedure for the polyorganoborosilazane T2-1.

The synthesis procedures were performed in argon atmosphere using the Schlenk technique. Borane dimethyl sulfide (2 M solution in toluene) was obtained from Sigma Aldrich GmbH, Germany. Dichloromethylvinylsilane (ABCR GmbH, Germany) was distilled from Mg freshly before use. Tetrahydrofurane and toluene were purified by distillation from potassium.

For the synthesis of tris(dichloromethylsilylethyl)borane (1), to a solution of 846 g (6 mol) dichloromethyvinylsilane in 900 ml toluene, 1000 ml of a 2 M solution of $H_3B.SMe_2$ were added at 0 °C in 6 h under vigorous stirring. The mixture was then stirred overnight at room temperature. After evaporation of SMe_2 and the solvent under reduced pressure, the compound was dried at 60 °C in vacuum ($4x10^{-2}$ mbar). A colorless, oily liquid was obtained, the yield was 870 g (99%). Chemical analysis provided the following composition [wt.%, exp(calc)]: Si 19.0 (19.2), B 2.5 (2.5), C 24.8 (24.7), H 4.3 (4.8), and Cl 48.5 (48.7).

For the synthesis of $<B\ [(C_2H_4)Si(CH_3)NH]_3>_n$ (2), 'T2-1', 600 g (1.4 mol) of (1) were dissolved in 900 ml tetrahydrofurane in a 4l Schlenk flask with gas inlet tube, mechanical stirrer, inside thermometer and reflux condenser. A stream of ammonia was introduced under vigorous stirring. The temperature raised up in 3 h to the boiling point; ammonia was introduced for 6 h. The mixture was filtered at room temperature thought a Whatman glass microfibre filter (GF/D). The filtrate was concentrated and dried in vacuum (8 Pa) at 80°C. 296.3 g (80 %) of a white solid was obtained.

To obtain an infusible precursor a heat treatment to cross-link and a solid state distillation to remove the remaining low molecular part was applied to **(2)**. 124 g of **(2)** were heated in a solid-state distiller 1 h at 250 °C in argon at normal pressure, then heated up to 350 °C at reduced pressure (6 Pa) and kept at these conditions for 5 h. This distillation separates 44.2 g (35.6%) of distillate, a high viscous oil, from 74.1g (59.7%) residue, a infusible white solid. For the following experiments only the infusible solid was used. Chemical analysis provided the following composition of the material [wt.%, exp.(calc)]: Si 32.1 (31.3), B 4.2 (4.0), C 40.1 (40.1), N 15.7 (15.6), H 7.2 (8.9), and O 0.8 (0.0).

2.2.2 Processing of amorphous and nano-crystalline Si-B-C-N ceramics from T2-1

The precursor polymer lumps were milled in argon using a tungsten carbide ball mill and sieved into various size fractions. Polymer particles in the size range 80 μm – 160 μm and polymer particles in the size range 32 μm – 80 μm were separated and compacted in a graphite die at 48 MPa uniaxial pressure in the temperature range 250 °C – 340 °C. The warm pressing temperature needed to be optimized to get dense green bodies. Before optimizing the warm pressing temperature for consolidation of the polymer particles into green bodies, it was required to determine the softening point of the polymer, in order that the first iteration for the warm pressing temperature is close to the optimum. To facilitate that, thermomechanical analysis was carried out on the polymer. A plot showing the displacement measured in micrometres as a function of temperature is given in Figure 2.5.

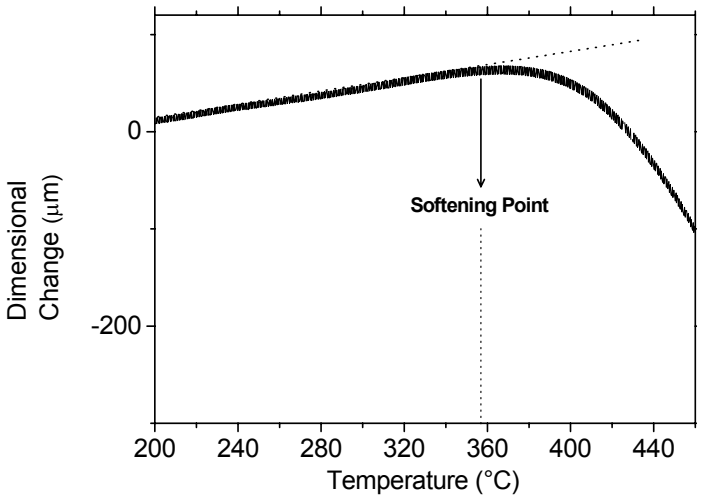

Figure: 2.5 Thermomechanical analysis of T2-1 polymer to determine the softening point.

Table 2.3 and 2.4 give details about how it was possible to arrive at the optimized warm pressing temperature as a function of the size of polymer particles.

It was clearly seen that the optimum warm pressing temperatures for the consolidation of the polymer particles in the size range 80 μm – 160 μm and 32 μm – 80 μm were **330 °C** and **280**

°C, beyond which the ceramics would crack and break into pieces after pyrolysis, as shown in Figure 2.6.

Warm pressing temperature [°C]	Weight of green body [g]	Weight of pyrolysed body [g]	Weight loss during pyrolysis [wt%]	Bulk density [g/cm^3]
250	1.992	1.4065	30	1.5663
280	1.992	1.4097	30	1.6786
320	2.500	1.7491	30	1.8446
330	1.649	1.1673	30	1.8917
340	**Broken after pyrolysis**			

Table: 2.3 Trial runs to determine the optimum warm pressing temperature for obtaining dense polymer green bodies which can lead to crack free amorphous ceramics (polymer particles size range used is 80 μm – 160 μm).

Warm pressing temperature [°C]	Weight of green body [g]	Weight of pyrolysed body [g]	Weight loss during pyrolysis [wt%]	Bulk density ρ [g/cc]
250	2.484	1.7477	30	1.92
280	2.505	1.7609	30	1.99
300, 320, 330	**Broken after pyrolysis**			

Table: 2.4 Trial runs to determine the optimum warm pressing temperature for obtaining dense polymer green bodies which can lead to crack free amorphous ceramics (polymer particles size range used is 32 μm – 80 μm).

(a) **(b)**

Figure: 2.6 Pyrolysed amorphous Si-B-C-N ceramics (a) Bulk body obtained using optimum warm pressing temperature (T_{opt}) (b) Pieces broken when the warm pressing temperature was > T_{opt}.

A weight loss of around 30 % was observed during pyrolysis (conversion of organic polymer to inorganic amorphous ceramics) which was independent of the size of the polymer particles used and also of the warm pressing temperature. A continuous increase in density with the increase in the warm pressing temperature was observed for both the cases. A maximum density of around 1.89 g/cm^3 and 1.99 g/cm^3 could be achieved after pyrolysis without any noticeable cracks (Table 2.3 and Table 2.4), i.e., the achievable density is a function of the size of polymer particles that are used.

The polymer green bodies were subjected to solid state thermolysis at a temperature of 1300 °C for 2 h in argon atmosphere. Upon pyrolysis, the polymer converts into an inorganic amorphous ceramic, which is accompanied by the evolution of gaseous species. The amorphous ceramics were then annealed in a high temperature furnace (FCT, Germany) to produce nano-crystalline ceramics. Annealing of all amorphous Si-B-C-N ceramics was done in nitrogen atmosphere. The following three different annealing treatments were carried out to study the influence of the temperature and holding time on the crystallization behavior. The applied nitrogen overpressure was held constant at 1 MPa in all cases.

- 1800 °C, 3 h at 1 MPa N_2
- 1900 °C, 3 h at 1 MPa N_2

- 1800 °C, 10 h at 1 MPa N_2

These annealing treatments were carried out for amorphous ceramics obtained from polymer particles in the size ranges 80 μm – 160 μm and 32 μm – 80 μm to study the influence of the size of the polymer particles on the crystallization behavior and also subsequently the high temperature deformation behavior. All the annealing treatments involved a heating schedule of 10 K/min till 1100°C, 4 K/min till 1300 °C and then 2 K/min till the desired annealing temperature. A cooling schedule of 5 K/min till 1300 °C followed by 20 K/min until room temperature was adopted.

2.3 Methods used for characterization

2.3.1 Nuclear magnetic resonance spectroscopy (NMR)

NMR experiments were carried out with a Bruker MSL spectrometer operating at a static magnetic field of 7.05 T (^{1}H frequency: 300.13 MHz) using a 4 mm magic angle spinning (MAS) probe. ^{13}C, ^{29}Si and ^{11}B NMR experiments were done at 75.47 MHz, 59.6 MHz and 96.26 MHz, respectively. ^{13}C and ^{29}Si NMR spectra were recorded under MAS conditions (sample rotation frequency: 5 kHz) with single pulse excitation, using π/2 pulse widths of 4.0 μs (^{13}C, ^{29}Si) and recycle delays up to 5 min. ^{29}Si and ^{13}C chemical shifts were determined relative to the external standards Q_8M_8, the trimethylsilylester of octameric silicate, and adamantane, respectively. These values were then expressed relative to the reference compound TMS (δ = 0 ppm). ^{11}B MAS NMR (central transition) spectra were recorded with single pulse excitation using π/6 (pulse length: 1.2 μs) pulses as well as recycle delays of 2s and a sample rotation frequency of 10 kHz. The spectra were calibrated relative to an aqueous solution of H_3BO_3 (δ =19.6 ppm) as external standard and are given relative to $BF_3{\cdot}OEt_2$ (δ = 0 ppm).

2.3.2 X- ray diffraction (XRD)

The XRD measurements were carried out on specimens obtained under four different annealing conditions using a SIEMENS D5000 X-ray diffractometer with a position sensitive detector and Cu Kα radiation. The voltage and current used for the measurements were 40 kV and 30 mA respectively.

2.3.3 Scanning electron microscopy (SEM)

SEM studies on crystallized Si-B-C-N ceramics before and after creep were carried out using a field emission microscope Zeiss DSM 982 GEMINI coupled with an EDX system (Oxford/Link ISIS 300) with a Germanium detector. SEM investigations were also carried out on plasma etched crystallized samples to observe the nano-crystallites and also micrometer sized crystallites in the pores and cracks. To observe the micrometer sized crystallites in the pores and cracks it was found that the optimized etching time in an equimolar CF_4/O_2 plasma was around 3.5 min, and samples which were over-etched (5 min) showed damaged crystals in the pores. All the samples were given a ~1.8 nm thick Pt-Pd coating before observation.

2.3.4 Transmission electron microscopy (TEM)

For TEM observations, samples were prepared following standard techniques, which involve diamond cutting, ultrasonic drilling, mechanical grinding, dimpling, polishing, and argon-ion thinning to perforation. TEM observations were made using a Philips CM200 microscope with an operating voltage of 200 kV.

2.3.5 Energy filtering transmission electron microscopy (EFTEM)/Electron spectroscopic imaging

EFTEM was carried out using a Zeiss EM 912 Ω microscope (with LaB_6 cathode operating at 120 kV) microscope which is specially designed to image the microstructure or the diffraction

patterns of the sample with electrons which have lost a certain amount of energy. This is done by incorporating an imaging energy filter into the projector system of the microscope. The filter works like a magnetic spectrometer, where electrons with different energies are differently deflected by the Lorentz force. Due to the special arrangement of the four magnets the filter is able to both introduce energy dispersion and, at the same time, transport the image information. For elemental mapping the data acquisition was performed with a water cooled Gatan 1024 X 1024 slow scan CCD camera with the Gatan software digital micrograph 2.5. Electron spectroscopic imaging was performed using the three-window method (Edgerton; two for the background and one to acquire the chosen element signal).

2.4 Chemical analyses – Elemental composition of materials

The chemical analyses of the polymers and henceforth the ceramics were carried out by using several techniques. Combustion techniques using Elementar Vario EL, ELTRA CS 800 and LECO TC 436 instruments, were carried out to determine carbon, nitrogen, hydrogen and oxygen in the materials investigated. Elementar Vario EL uses an oxygen jet which is directly injected at the sample and the combustion conditions are controlled and as well as the furnace temperatures till 1200 °C to ensure complete combustion. A special low-noise thermoconductivity cell serves as detector in the entire dynamic detection range.

ELTRA CS 800 C/S determinator is also used to determine the carbon content in the materials. The equipment is supplied with infrared cells whose sensitivities with respect to the IR-absorbtion lengths can be individually selected to offer optimum precision for the analysis of high and low levels of carbon. The CS 800 features a 16-bit microprocessor, an induction furnace and solid state infrared detectors with auto zero and auto range control.

Using LECO TC 436, quantitative determination of nitrogen and oxygen can be made by reaction of oxygen in the sample at high temperatures (700 – 2700 °C) with carbon, forming CO_x, and thermal release of molecular nitrogen in the electrically heated furnace; selective CO

and/or CO_2 detection is done by infrared absorption and nitrogen is measured by thermal conductivity.

2.4.1 Inductively coupled Plasma – Atomic emission spectroscopy (ICP-AES)

ICP-AES is carried out using an ISA JOBIN YVON JY70 plus instrument for the determination of boron in the crystalline Si-B-C-N ceramic materials. ICP-AES uses a gas discharge where the specific elements emit light, a spectrometer which separates the characteristic wavelengths and a detector. The sample to be analyzed is introduced into the spectrometer after dissolution. A plasma source is used to dissociate the sample into its constituent atoms or ions, exciting them to a higher energy level. They return to their ground-state by emitting photons of a characteristic wavelength depending on the element present. This light is recorded by an optical spectrometer. When calibrated against standards the technique provides a quantitative analysis of the sample.

2.4.2 X-ray fluorescence

When a primary x-ray from an x-ray tube or a radioactive source strikes a sample, the x-ray can either be absorbed by the atom or scattered through the material. If the primary x-ray had sufficient energy, electrons are ejected from the inner shells, creating vacancies. These vacancies present an unstable condition for the atom. As the atom returns to its stable condition, electrons from the outer shells are transferred to the inner shells and in the process give off a characteristic x-ray whose energy is the difference between the two binding energies of the corresponding shells. Because each element has a unique set of energy levels, each element produces x-rays at a unique set of energies, allowing one to measure the elemental composition of a sample. The process of emissions of characteristic x-rays is called x-ray fluorescence, or XRF. Analysis using x-ray fluorescence is called *X-ray Fluorescence*

Spectroscopy. The XRF method is widely used to measure the elemental composition of materials. Here in this work, the method is used to determine silicon in the ceramic materials.

2.5 Ultrasonic phase spectroscopy for Young's modulus measurements

Si-B-C-N ceramics were synthesized with tailored porosities i.e., densities ***by controlling the warm pressing temperature*** used for the consolidation of the polymer particles into a green body. Si-B-C-N ceramics obtained with four different porosity levels (density levels) were considered for investigation. Elastic properties were measured for ceramics obtained from polymer particles in the size range of 80 μm – 160 μm and 32 μm – 80 μm to study the influence of the size of the polymer particles on the elastic properties. Processing of such nano-crystalline ceramics has been described earlier (Section 2.2.1) . All the ceramics whose elastic properties had to be determined were cut into four parts, as shown in Figure 2.7. One part remained amorphous and the other three parts were annealed at 1800 °C, 1900 °C and 2000 °C in a nitrogen atmosphere of 1 MPa for 3 h (Figure 2.7).

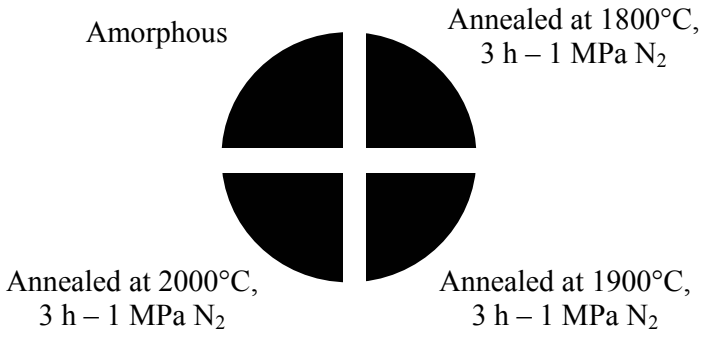

Figure: 2.7 Samples cut into four quadrants and heat treated at different temperatures.

The amorphous and all the annealed ceramics were subjected to ultrasonic phase spectroscopy to measure the velocities of the ultrasonic waves passing through the specimens.

2.5.1 Measurement procedure

A schematic sketch of the experimental set up for the measurement of the elastic properties of specimens is shown in Figure 2.8. Two ultrasonic transducers of the same kind are attached to opposite sides of a specimen with parallel planar faces. One transducer is used to transmit a continuous, harmonic elastic longitudinal wave into the specimen, the other one is used to receive the signal transmitted through the specimen. The phase angle as well as the magnitude of the input and output electronic signals are measured. For the measurements, the transducers were held on either flat side of the specimen using a sugar syrup as a couplant. A Hewlett Packard HP4195A network analyzer was used which allows magnitude measurements over a dynamic range of around 100 dB at a resolution of 0.001 dB and phase comparison measurements over a range of ± 180° at a resolution of 0.01°. The instrument can be operated in the frequency range of 10 Hz – 500 MHz.

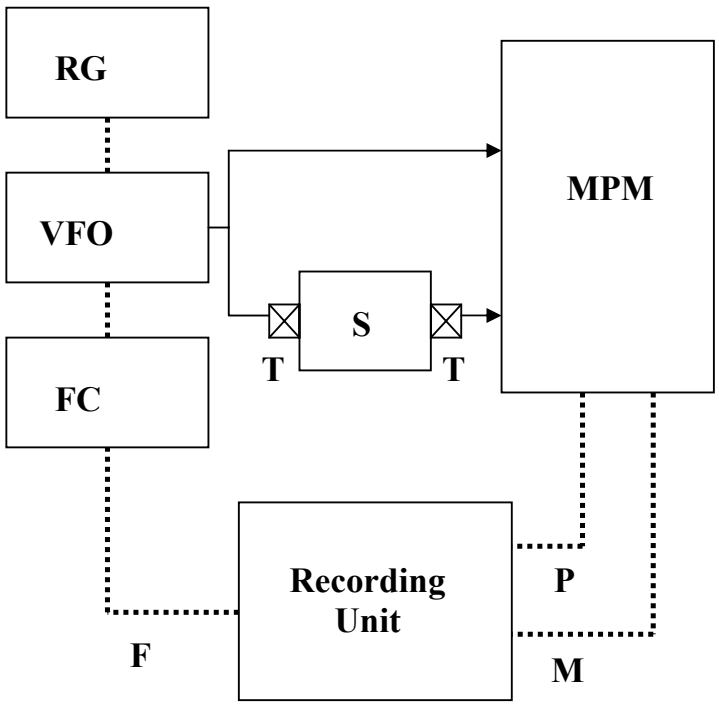

Figure: 2.8 Schematic of the experimental set-up for ultrasonic measurements (RG = Ramp generator, VFO = Variable frequency oscillator, FC = Frequency counter, MPM = Magnitude and phase meter, S = specimen, T = Transducer, F = Frequency, P = Phase, M = Magnitude) [98Wan].

2.6 Creep

To provide useful engineering data, long term high temperature mechanical testing of ceramics must incorporate strict temperature control (± 5°C); accurate temperature measurement (1 percent of the nominal temperature); close control of grip cooling (± 0.1°C); and responsive data acquisition systems. When these aspects are closely controlled and monitored, creep tests can be reliably conducted to nearly 5000 h with measured minimum creep strain rates as low as 10^{-10} s^{-1} at 1400 °C, which is in the range of physically measurable rates.

Creep specimens with nominal dimensions of 3 mm x 3 mm x 7 mm were cut from the ceramic monoliths followed by grinding to make all the six faces of the specimens parallel to each other. Compression creep tests were performed at 1400 °C in air at a compressive stress of 100 MPa for constant load experiments. Most of the creep tests were restricted to testing time frames of 100 – 300 h depending on the material being tested and requirements. The displacements measured during compression creep are plotted on the positive direction of the y-axis.

Load change experiments with the schedule shown in Table 2.5 were restricted to amorphous and crystallized Si-B-C-N ceramics derived from MW – 33 polymer precursor. The compression creep experiments were carried out using a testing frame from *Amsler*, having a force range of 0.5 – 5 kN with an accuracy of ~ ± 1 N. The temperature was measured with a Pt Rh(10)/Pt thermocouple.

Time (s)	Stress (MPa)
0 - 2.5×10^5	100
2.5×10^5 - 5×10^5	150
5×10^5 - 9×10^5	200
9×10^5 - 1×10^6	5

Table: 2.5: Load-time schedules for carrying out load change experiments to determine the viscosity and analyze the anelastic behavior.

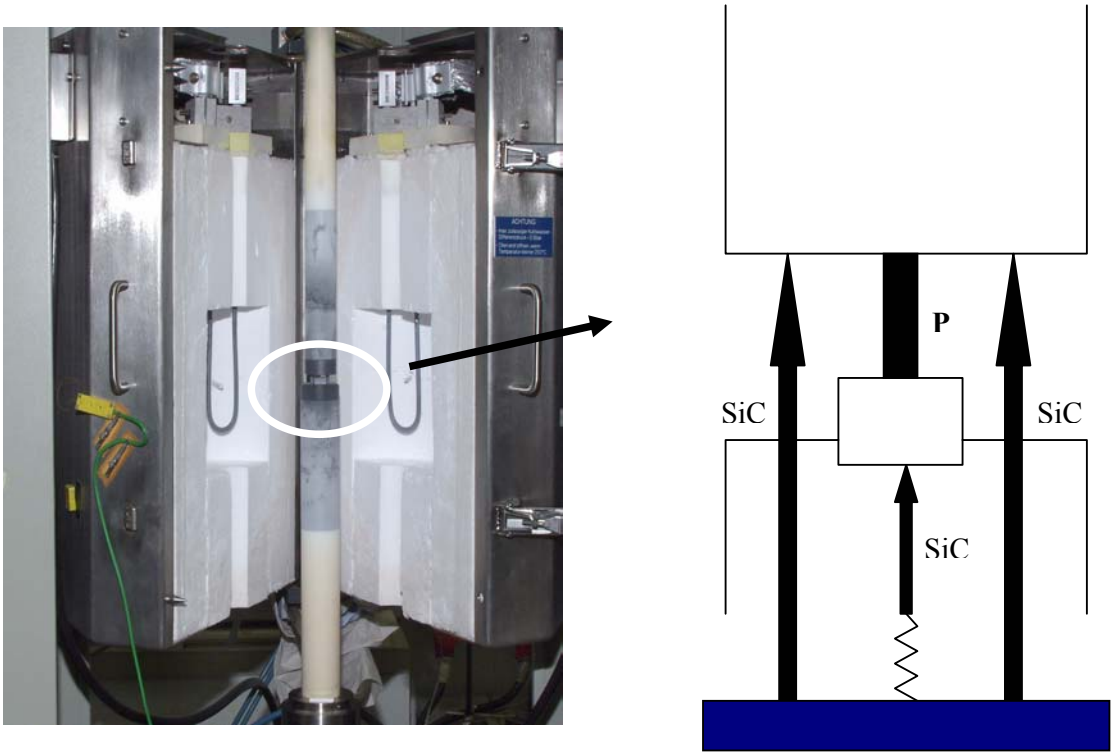

Figure: 2.9 Experimental set-up for compression creep experiments with a schematic sketch on the right side showing SiC scanning pins used for displacement measurements and the specimen P under compression.

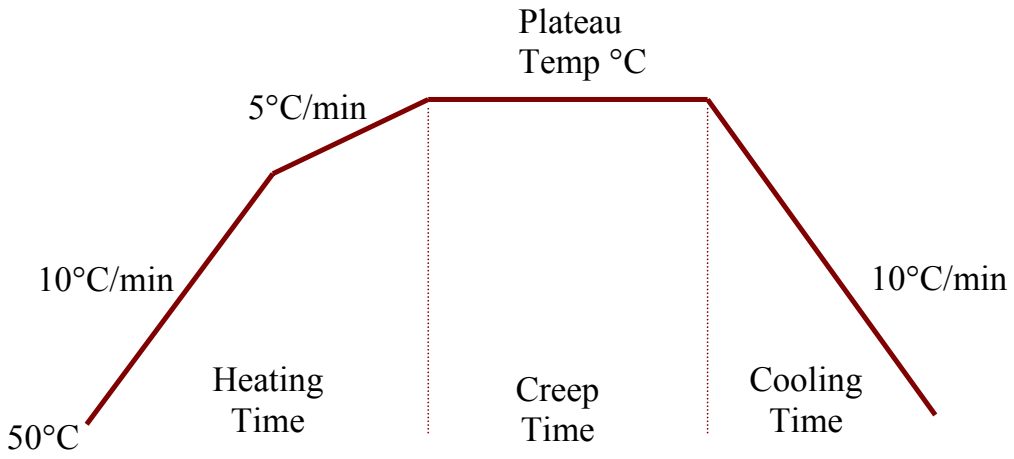

Figure: 2.10 Heating and cooling schedules in a typical compression creep experiment.

The load was applied by a spiral spring, which was preloaded by a spindle. The compression of the spiral spring was measured by a linear potentiometer. The strain of the specimen was calculated from the displacement of the load pads. Two SiC scanning pins connected the

upper load pad with the housing of an inductive strain gauge, which was placed under the specimen outside of the furnace in the cold part of the testing machine. The displacement between the upper and lower load pad was measured with a third scanning pin, which connected the sensor of the strain gauge with the lower load pad. The experimental setup is shown in Figure 2.9.

The typical heating and cooling schedule in a compression creep experiment is shown in Figure 2.10. T2-1 derived crystalline Si-B-C-N ceramics were investigated using a test frame from *Zwick*; these materials were investigated in the temperature regimes of 1350 °C – 1500 °C, with constant compressive loads varying from 5 MPa – 100 MPa.